Hannah Combs
Department of Biomedical Engineering,
The University of Akron,
Akron, OH 44325

Taylor Shark
Department of Biomedical Engineering,
The University of Akron,
Akron, OH 44325

Jacob Heiss
Department of Biomedical Engineering,
The University of Akron,
Akron, OH 44325

Mehdi Raessi
Department of Mechanical Engineering,
University of Massachusetts Dartmouth,
Dartmouth, MA 02747

Hossein Tavana[1]
Department of Biomedical Engineering,
The University of Akron,
260 South Forge Street,
Akron, OH 44325
e-mail: tavana@uakron.edu

A Quantitative Study of Transport of Surfactant Boli in a Three-Dimensional Lung Model of Neonates

Neonatal respiratory distress syndrome is mainly treated with the intratracheal delivery of pulmonary surfactants. The success of the therapy depends on the uniformity of distribution and efficiency of delivery of the instilled surfactant solution to the respiratory zone of the lungs. Direct imaging of the surfactant distribution and quantifying the efficiency of delivery is not feasible in neonates. To address this major limitation, we designed an eight-generation computational model of neonate lung airway tree using morphometric and geometric data of human lungs and fabricated it using additive manufacturing. Using this model, we performed systematic studies of delivery of a clinical surfactant either at a single aliquot or at two aliquots under different orientations of the airway tree in the gravitational space to mimic rolling a neonate on its side during the procedure. Our study offers both a novel lung airway model and new insights into effects of the orientation of the lung airways and presence of a pre-existing surfactant film on how the instilled surfactant solution distributes in airways. [DOI: 10.1115/1.4055428]

Keywords: neonatal respiratory distress syndrome, lung airway model, plug flow, liquid plug splitting, distribution index, efficiency index, deposition volume

Introduction

The lungs contain a continuously branching network of airways that begin at the trachea (airway generation $z = 0$) and divide into five lobes, extending to the terminal bronchioles by dichotomous branching at each bifurcation [1,2]. The airways reduce in diameter and length but increase in number as they penetrate deeper into the lungs and terminate in alveoli [2]. Due to their small, submillimeter size scale, alveoli are prone to surface tension-driven instabilities during breathing [2]. Type II alveolar epithelial cells synthesize and secrete a pulmonary surfactant that forms a lipid monolayer at the air-liquid interface of alveoli and respiratory bronchioles to reduce the air-liquid surface tension and stabilize them [2–6].

Preterm infants born before 28 weeks of gestation often lack or have inadequate production of natural surfactant because their lungs are underdeveloped [7]. This may result in neonatal respiratory distress syndrome where high surface tension forces collapse the respiratory units and cause labored breathing [8]. To address this problem, an exogenous surfactant solution is instilled into the trachea to form a liquid plug, which is set in motion using mechanical ventilation [9,10]. The plug divides at each airway bifurcation and splits at a ratio dependent on gravitational and fluid flow forces [11]. As the resulting plugs propagate, they deposit a trailing film onto the airway walls, reduce in volume, and finally rupture. The deposited film drains by gravity and through surface tension gradients toward the alveoli [12]. The success of neonatal surfactant replacement therapy (NSRT) depends on a uniform surfactant delivery to most of the lung [13,14]. This is largely determined by the efficiency and distribution of the instilled volume. The efficiency determines the proportion of the instilled dose to reach the alveoli, whereas the distribution refers to where in the lung the surfactant reaches [15].

While NSRT is a life-saving strategy, there is no consensus about the position of a baby during the procedure, number or volume of aliquots, and the time interval between them. A major obstacle is inadequate understanding of transport of instilled surfactant in airways. Inaccessibility of airways hinders direct observation of surfactant delivery in the airway tree. A clinical limitation is the inability to safely image preterm infants' lungs during or after the procedure [15]. As a result, NSRT procedures are quite inconsistent and based on the practitioner's experience: Treatments may involve instilling surfactant in four quarter-dose or two half-dose aliquots with arbitrary 1–10 min intervals [16–18]. The baby may be placed on the back and inclined up or down or rotated partially or fully to the sides [19]. The success of NSRT is evaluated indirectly through the neonate's respiration rate and oxygen levels [20]. A fundamental understanding of surfactant transport in airways is critical to improve NSRT.

To address this need, various computational studies have been conducted. Most studies have used simple models that represent a single airway tube, a single bifurcation, or planar microfluidic models with a few airway generations [11,21–24]. Although these models provided insight into mechanisms of film deposition from plugs, effects of surfactant type and fluid mechanical forces, and interactions of moving fluid with the airway walls, they were inherently limited in studying surfactant transport in the lung airway tree during NSRT. To overcome this limitation, a three-dimensional (3D) mathematical lung model was used to evaluate the efficiency and homogeneity of surfactant delivery in the lung [15].

There is currently a lack of physical models to facilitate experimental studies of transport in lung airways. We recently addressed this need by computationally designing an eight-generation model of the lung airway tree of neonates using morphometric measurements of human lungs scaled to the size of a neonate lung and fabricating physical models using additive manufacturing [25]. We showed the feasibility of imaging surfactant solutions in this semi-transparent lung airway tree model for quantitative studies. Leveraging this novel model, here we examined the efficiency and distribution of a clinical surfactant as a single aliquot and two aliquots. We found that rolling the model away from a horizontal position during a single aliquot delivery led to a significantly greater surfactant volume in the gravitationally favored lung. Additionally, the presence of a pre-existing surfactant film from a

[1]Corresponding author.
Manuscript received April 12, 2022; final manuscript received August 15, 2022; published online October 6, 2022. Assoc. Editor: Ethan Kung.

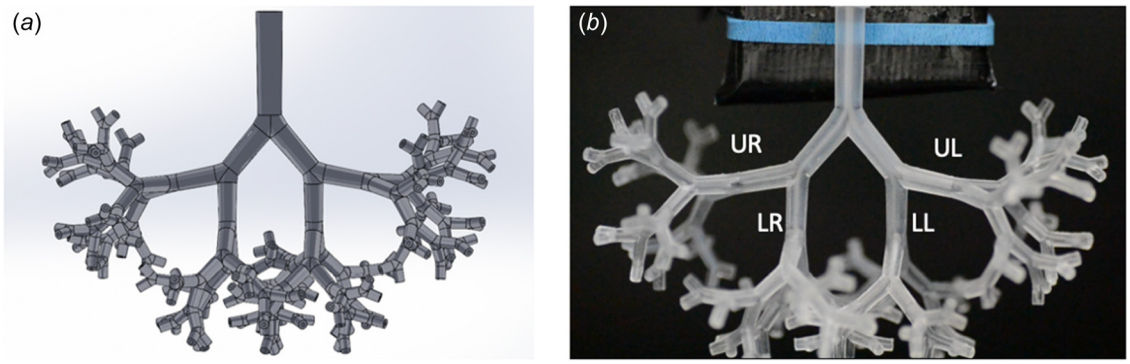

Fig. 1 (*a*) A computational model of an eight-generation airway tree and (*b*) the corresponding fabricated model with labeling for four lobes at $z = 2$ as UR, LR, LL, and UL are shown

previous instillation significantly increased the efficiency of surfactant delivery to lower airways in the model. Our engineered lung airway model provides a tool for quantitative studies of transport of liquid boli or aerosolized solutions of different fluids in airways [26].

Materials and Method

Working Fluid. Infasurf (ONY, Inc., Getzville, NY), a natural Calfactant with a phospholipid concentration of 35 mg/mL, was generously provided by the manufacturer and used. The properties of Infasurf include a surface tension of $\gamma = 25$ dynes cm^{-1} and a density of $\rho = 0.980$ g cm^{-3} [6,25].

Experimental Setup and Liquid Plug Generation. Neonatal lung airway models were designed in SOLIDWORKS as we previously described [25]. The model containing eight generations, i.e., 255 airway tubes, was fabricated using a semitransparent material to allow for imaging of surfactant plugs during plug propagation (Fig. 1). The model was anchored to a Plexiglas platform clamped on a Panavise [11]. An accelerometer allowed for accurate adjustments of the roll angle (α) using the Panavise. Altering the roll angle simulated the placement of a preterm infant in the supine position ($\alpha = 0$ deg) and gradually rolling to the right lateral decubitus position ($\alpha = 90$ deg) (Fig. 2). Experiments were conducted at $\alpha = 0$ deg, 30 deg, 60 deg, and 90 deg. Before experiments, each model was treated with a high frequency oxygen plasma (Harrick Plasma) for 10 min to render the airways hydrophilic [10]. A 280 μL plug of distilled water was placed in the tracheal tube and propagated through all airways to prewet the airways. The residual water was aspirated from the end of all terminal airways while allowing a thin film of water to remain in all airways. For the single-aliquot studies, a 140 μL plug of Infasurf was instilled into the tracheal tube using a positive displacement pipette. The tracheal tube was connected to a syringe pump (Chemyx Inc., Stafford, TX) using silicon tubing (Tygon) on a plastic syringe (Norm-Ject). Forced air was used to propagate the plug through the airways. A similar procedure was followed for the two-aliquot experiments. A 140 μL surfactant plug was instilled through the lung model, the remaining of the first aliquot was aspirated from the end of terminal airways, and a second 140 μL aliquot was placed inside the tracheal tube and set in motion using airflow.

Imaging, Image Analysis, and Statistical Analysis. Videos of experiments were recorded at 30 fps from three views (Movie S1–S3 available in the Supplemental Materials on the ASME Digital Collection). The top view was recorded using a Nikon D3100 with a macrolens (Tamron 272ENII, 90 mm). The front view was recorded using a Canon T6 rebel with a macrolens (Canon EF-S, 55 mm). The side view was recorded using a cell phone (Samsung Galaxy A20). Videos were imported into IMAGEJ (NIH) and trimmed to the same number of frames to quantify plug volumes in airways. The distances of the plug from the top (X_1) and bottom (X_2) of each airway and the length of the plug ($P\iota$) were measured (Fig. S1 available in the Supplemental Materials). These values were added to obtain the total measured length of each airway tube. This length was compared against the known length of the airway to verify accurate measurements for volume calculations. The plug length was used to calculate the volume of each plug inside different airways. A distribution index (DI) was defined as the volume of surfactant solution that enters each of the four lobes of the airways to the instilled volume. An efficiency index (η) was defined as the percentage of the instilled dose to reach the fifth-

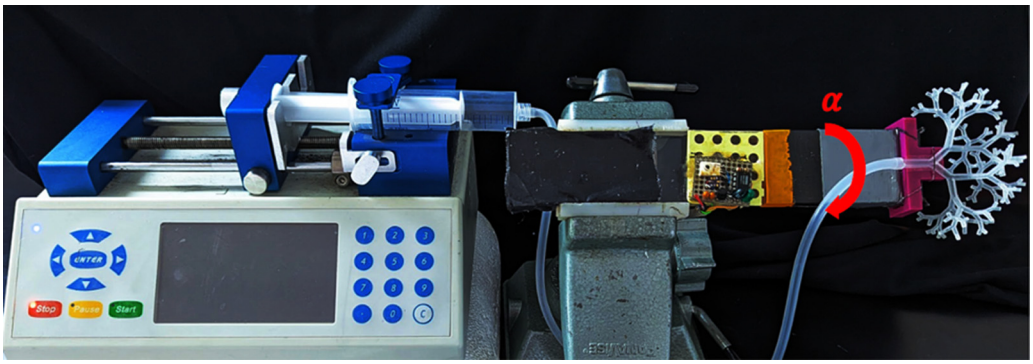

Fig. 2 Experimental setup consisting of a syringe pump connected to the lung airway model using Tygon tubing. A Panavise is used to modify the roll angle quantified using an accelerometer on the platform. The airway model is fixed on an in-house clamp. The arrow shows the rotation of the airway model using the roll angle.

generation airways due to the feasibility of clearly imaging surfactant plugs in these airways. Experiments at each orientation had four replicates to evaluate effects of roll angle and a pre-existing film on the distribution of surfactant and efficiency of delivery. Statistical significance was determined using a one-way analysis of variance paired with an least significant difference posthoc test ($p < 0.05$).

Quantifying the Distribution Index. The four lobes emerging at $z = 2$ generation were labeled as the upper right (UR), lower right (LR), lower left (LL), and upper left (UL) (Fig. 1(*b*)) [1]. The volume of plugs inside each of the four lobes was calculated as $V = \frac{\pi}{3} P_l \left((r_1^2 + r_2^2) + (r_1 \times r_2)\right)$, where r_1 and r_2 are the radii of $z = 2$ airway where the top and bottom of each plug are located. The change in airway radius is caused by the tapering geometry of each airway [1]. Using this process, the volumes of surfactant plugs at each of the four lobes were determined (Fig. S1 available in the Supplemental Materials on the ASME Digital Collection) to calculate DI for each lobe using $DI = V_{z=2}/V_{z=0}$ at different roll angles. Compared to human lungs which contain five lobes, our model contains four lobes. This is because of the symmetric design that includes the airways of the middle right lobe within the LR lobe.

Estimating Volumes of Stagnant Plugs. Measuring of plug lengths and quantifying plug volumes was also done for $z = 3$, 4, and 5 airways. As the lung model was rolled laterally, the UR and LR regions became gravitationally favored, causing a decrease in the volume of the plugs that were delivered to the LL and UL lobes. At $\alpha = 30$ deg and 60 deg, small plugs that propagated to the left lung ruptured in $z = 1$ to $z = 2$ airways, allowing the forced air to move freely into the left lobes and causing the remaining surfactant plugs to stop in $z = 3$ airways. Estimated volume loss due to film deposition and plug splitting were completed for stagnant plugs to facilitate quantifying the volume of surfactant that would have been delivered to $z = 5$. To estimate volume loss, a surfactant plug was propagated through individual tubes representing each of $z = 0$–4 airways. The initial and final plug volumes were determined and the volume loss over a travel distance, d, was found as $V_L = (V_1 - V_2)/d\ (\mu\text{L/mm})$. The single tube experiments were completed considering the geometry of the corresponding bifurcation zones in the airway tree that contains a +40 deg or –40 deg angle from the centerline of their parent airway tube, causing different volume losses in anterior and posterior daughter tubes. The plug split ratio was used to estimate if the stagnant plug would have entered the anterior or posterior airways after traveling through the bifurcation zone [11].

Quantifying the Efficiency Index at Different Roll Angles. An efficiency index (η) was defined as the percentage of the instilled dose delivered to the fifth-generation airways and calculated using $\eta = 100 \times \sum_{i=1}^{32} V_{5,i}/V_0$, where V_0 was the instilled volume in the trachea and V_5 was the total volume of plugs in $z = 5$ airways. η was calculated for a single aliquot at $\alpha = 0$ deg, 30 deg, 90 deg and for a second aliquot at $\alpha = 0$ deg, –30 deg, –90 deg. The positive and negative roll angles simulate the delivery of the first and second aliquots while rotating the neonate.

Results

Airway Models and Testing Platform. We designed the airway models in SOLIDWORKS (Fig. 1(*a*)). To approximate an infant's trachea [1,25], we created a 3.5 mm-diameter circle and extended it to 17.5 mm while tapering down its diameter by 13.5%. We calculated the average diameter of subsequent generations using $d_z = d_0 \times 2^{-z/3}$, where d_0 is the tracheal diameter and z is the generation number [1]. The lengths of the tracheal tube and all other airways were estimated using $l_0 = 5d_0$ and $l_z = 3d_z$, respectively [1]. The bifurcation angle between each two daughter airways was $\theta = 80$ deg [27]. Starting at the generation $z = 3$, the airways rotated 90 deg to mimic anatomic rotation of airways inside the chest cavity. For single tube experiments, we designed 50 mm-long airway tubes to allow for the imaging of propagating plugs and calculating volume loss due to film deposition. The diameter of every single tube was designed to represent the corresponding airway in the multigeneration model, starting with $z = 0$ airway with a diameter of 3.5 mm and each subsequent generation decreasing in diameter according to $d_z = d_0 \times 2^{-z/3}$. We fabricated all models using a Viper si2 stereolithography system (3D Systems, Inc.) (Fig. 1(*b*)) [25]. The symmetric design of airways in our model led to four lobes, compared to five lobes in native lungs, which are asymmetric between the left and right sides. Nevertheless, we did not reduce the number of airways. The model still includes all the bifurcations and airways but in a symmetric geometry. Airways that would be in the middle lobe in the right lung appear in the LR lobe in our model.

Volume Loss From Propagating Surfactant Plugs. Propagating surfactant plugs in airways flow over a thin aqueous film that maintains the airway tissue hydrated. Propagating plugs lose mass by depositing a film from their trailing menisci onto the airways and eventually rupture. To quantify volume loss, we determined the initial and final plug volumes in single airway tube models representing different airway generations [25]. The tracheal tube was positioned only at $\alpha = 0$ deg because it remains in the same position despite rolling the model. The $z = 1$–4 tubes were positioned at $\alpha = 0$ deg in the supine position, at 40 deg, or at –40 deg. We selected these positions because each daughter tube in a bifurcation zone is oriented 40 deg from the centerline of its parent tube. We formed a 140 μL Infasurf plug in the tube and propagated it using an airflow rate of 30 mL/min for the tracheal tube and 15, 7.5, 3.75, and 1.875 mL/min for the first, second, third, and fourth generations, respectively. These flow rates resulted in the corresponding Capillary numbers (Ca) of 0.016, 0.013, 0.010, 0.008, and 0.006. $Ca = \mu u/\gamma$ represents the relative effects of viscous and surface tension forces, where μ and γ are, respectively, the dynamic viscosity and surface tension of the surfactant solution and u is the plug velocity. During the placement of the 140 μL Infasurf plug, the overall volume decreased by approximately 14 μL. We determined this loss in volume between the surfactant leaving the pipette tip and being placed in the trachea by weighing the pipette tip before the addition of the plug and after the plug was placed in the trachea. The difference in weight of the pipette tip was used to calculate the volume of surfactant left behind in the tip.

The largest volume loss occurred in the tracheal tube with $1.69 \pm 0.04 \mu\text{L/mm}$ (Fig. 3), translating into a dimensionless film thickness of 0.09 (Fig. S2 available in the Supplemental Materials). This was consistent with result from the classical Bretherton law for small Capillary numbers, i.e., $h/r = 1.34\text{Ca}^{\frac{2}{3}}$ [28], which gave a dimensionless film thickness of 0.08, but less so with a model for larger Capillary numbers, i.e., $h/r = 1.34\text{Ca}^{\frac{2}{3}}/\left(1 + 1.34 \times 2.5\text{Ca}^{\frac{2}{3}}\right)$ [29], which gave a dimensionless film thickness of 0.07. In the subsequent generations and at a 0 deg orientation, the volume loss progressively decreased and reached $0.12 \pm 0.01\ \mu\text{L/mm}$ at $z = 4$ (Fig. 3). The resulting dimensionless film thickness values at this orientation closely agreed with the theoretical estimation (Fig. S2 available in the Supplemental Materials). For the $z = 1$ airway tube, we found the largest and smallest volume losses at an orientation of 40 deg with $1.15 \pm 0.04\ \mu\text{L/mm}$ and at –40 deg with $0.58 \pm 0.07\ \mu\text{L/mm}$ and both were significantly different from that in a horizontal orientation ($p < 0.05$). While the effect of gravitational orientation on volume loss continued for generations $z = 2$, 3, and 4, it became less pronounced. For $z = 3$ and 4, the measured volume losses were independent of orientations of the airway tubes, indicating that the effect of gravitational force on film deposition from the

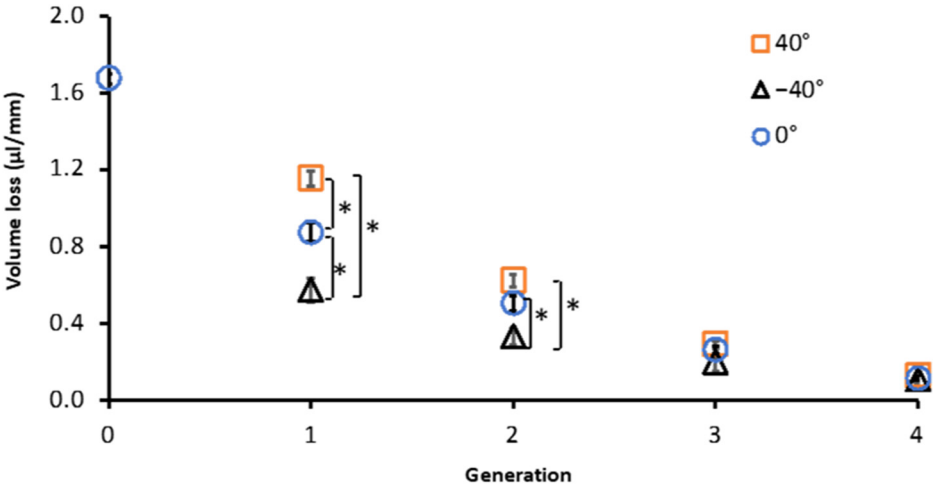

Fig. 3 Volume loss from surfactant plugs propagating in single tubes representing airway generations $z = 0$, 1, 2, 3, and 4 at different orientations. Each airway tube was 50 mm in length but with a similar diameter to its corresponding airway tube in the multigeneration model. *$p < 0.05$.

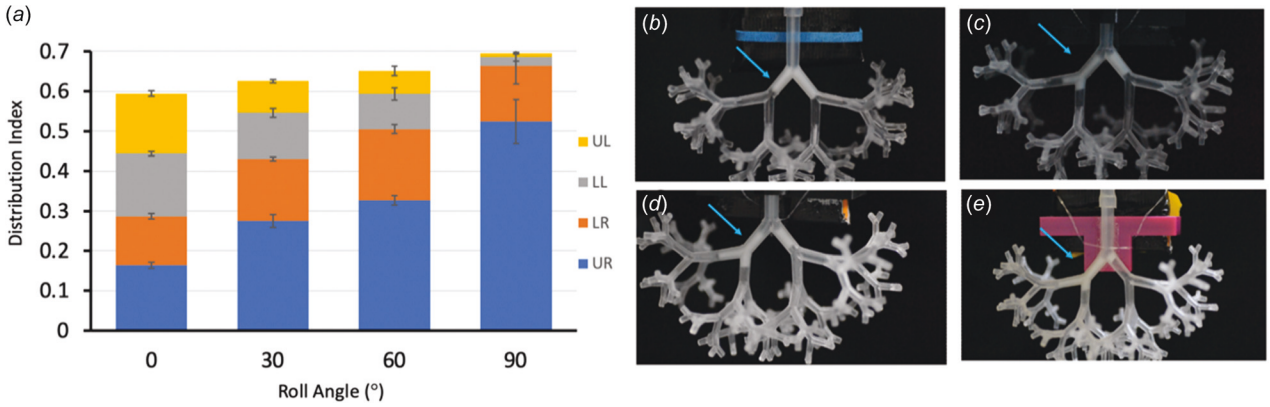

Fig. 4 (*a*) The distribution index for the UL, LL, LR, and UR lobes quantifies the effect of orienting the airway tree under various roll angles (α) on surfactant distribution in these lobes. Surfactant distribution at $z = 0$–1 bifurcation for (*b*) $\alpha = 0$ deg, (*c*) $\alpha = 30$ deg, (*d*) $\alpha = 60$ deg, and (*e*) $\alpha = 90$deg. Arrows in the images point to surfactant plugs.

plugs significantly reduces beyond generation $z = 2$, consistent with a 2.5-fold decrease in the Bond number from $z = 0$ to $z = 2$. The Bond number ($\mathrm{Bo} = \rho g D^2/\gamma$, i.e., the ratio of gravitational forces to surface tension forces) at $z = 2$ was 0.46.

Quantitative Analysis of Distribution of Single Aliquot Surfactant in Airways

Distribution Index and Efficiency Index. To study how lateral rotation of the lung could change surfactant distribution among different lobes, we oriented the airway models at roll angles of $\alpha = 0$ deg, 30 deg, 60 deg, and 90 deg, instilled an Infasurf plug in the tracheal tube and propagated it at $\mathrm{Ca} = 0.016$ [25], estimating the flow rates of $z = 1$–5 to be half of that of the previous generation. These orientations simulate the infant being rolled to their right side and away from the horizontal axis during NSRT. We quantified total plug volumes inside the UR, LR, LL, and UL lobes to calculate DI. At $\alpha = 0$ deg, the surfactant plug split fairly evenly among the four lobes, with $\mathrm{DI_{UR}} = 0.16 \pm 0.008$, $\mathrm{DI_{LR}} = 0.12 \pm 0.007$, $\mathrm{DI_{LL}} = 0.16 \pm 0.005$, and $\mathrm{DI_{UL}} = 0.15 \pm 0.007$ (Figs. 4(*a*) and 4(*b*)). The sum of the four indices did not add up to one due to volume loss from the plugs. Increasing the roll angle to $\alpha = 30$ deg made the UR lobe more gravitationally favored, significantly increasing the DI for the UR lobe to $\mathrm{DI_{UR}} = 0.28 \pm 0.016$ ($p < 0.05$) but slightly for the LR lobe to $\mathrm{DI_{LR}} = 0.16 \pm 0.005$ ($p < 0.05$). This was accompanied by a significant decrease in the volume of surfactant that traveled to the left side of the lung, reflected in $\mathrm{DI_{LL}} = 0.12 \pm 0.011$ and $\mathrm{DI_{UL}} = 0.08 \pm 0.004$ ($p < 0.05$) (Figs. 4(*a*) and 4(*c*)). Further increasing α to 60 deg led to a greater surfactant volume in the right lung with $\mathrm{DI_{UR}} = 0.33 \pm 0.012$ and $\mathrm{DI_{LR}} = 0.18 \pm 0.011$, and reduced volume in the left lung with $\mathrm{DI_{LL}} = 0.09 \pm 0.010$ and $\mathrm{DI_{UL}} = 0.06 \pm 0.012$ ($p < 0.05$) (Figs.4(*a*) and 4(*d*)). A roll angle of $\alpha = 90$ deg that simulated a neonate rolled onto their right side resulted in the delivery of majority of the surfactant solution to the right lung with $\mathrm{DI_{UR}} = 0.52 \pm 0.056$ ($p < 0.05$) and $\mathrm{DI_{LR}} = 0.14 \pm 0.044$, and minimal delivery to the left lung with $\mathrm{DI_{LL}} = 0.02 \pm 0.009$ and $\mathrm{DI_{UL}} = 0.01 \pm 0.002$ (Figs. 4(*a*) and 4(*e*)). Overall, a roll angle of 90 deg led to almost exclusive surfactant delivery to one side of the lung and the smallest volume loss on airway walls, which is evident from the largest cumulative DI of 0.7 (Fig. 4(*a*)).

Next, we determined the efficiency of surfactant delivery to $z = 5$ airways at these four orientations. This was due to the feasibility of quantifying plug volumes in this generation. We found an efficiency of $\eta = 42.1\% \pm 0.7$ for $\alpha = 0$ deg. When α increased to 30 deg and 60 deg, η only marginally changed to $41.3\% \pm 0.7$ and $45.9\% \pm 1.2$ ($p < 0.05$), respectively. However, at $\alpha = 90$ deg, η significantly increased to $58.2\% \pm 1.4$ ($p < 0.05$). This increase

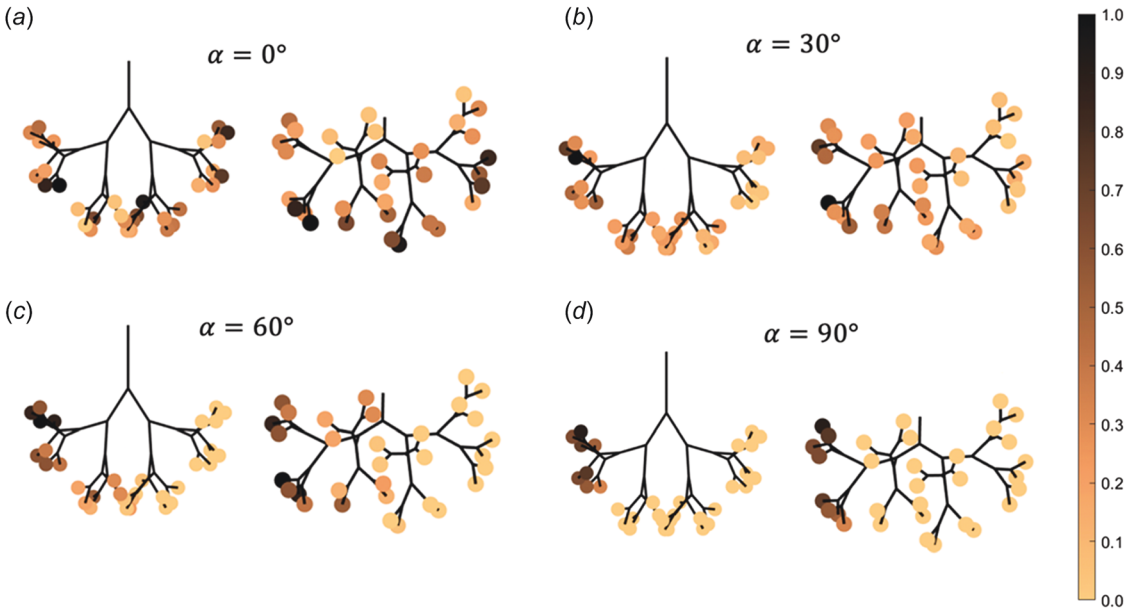

Fig. 5 Heatmaps representing surfactant distribution through the airway tree into the $z = 5$ generation airways at four different orientations in single aliquot experiments. Two different views of airways are shown at each orientation. The $z = 5$ airways are represented as colored spheres where the color bar defines the normalized surfactant solution volume in z = 5 airways.

was due to less surfactant solution loss on the walls because the plugs traveled fewer airways at this orientation.

Surfactant Distribution in Right and Left Lungs. Next, we determined the distribution of surfactant in the $z = 5$ airways of left and right lungs. At $\alpha = 0$ deg, the surfactant solution reached all airways of the lung, delivering 47.0% ± 1.4 of the total volume of surfactant inside of $z = 5$ to the right lung and 53.7% ± 1.64 to the left lung (Fig. 5(*a*)). While we expected a relatively equal distribution between left and right lungs, the small difference is likely due to experimental errors in finding plug volumes. Rolling the model 30 deg significantly increased the surfactant solution in $z = 5$ airways of the right lung to 75.8% ± 1.8 and decreased that in the left lung to 24.2% ± 1.8 (Fig. 5(*b*)). This asymmetric distribution further increased at $\alpha = 60$ deg to 91.6% ± 3.0 for the right lung and decreased to 8.4% ± 3.0 for the left lung (Fig. 5(*c*)). A complete asymmetric delivery occurred at $\alpha = 90$ deg with all the surfactant solution delivered to the right lung and 0% of the left lung (Fig. 5(*d*)). We note that although a small amount of surfactant solution entered the left lung at this orientation, it did not reach $z = 5$ airways due to volume loss on airway walls during plug propagation.

Effect of a Pre-Existing Surfactant Film on the Distribution Surfactant in Airways. In clinical settings, a single dose of surfactant may be divided into two or more aliquots and administered with the infant kept at the same orientation or rolled at different orientations, such as to the right and left [18,30,31]. Dividing the dose and rotating the infant is used to increase the likelihood of delivering surfactant to most of the lung. We divided a dose into two aliquots and quantified the volume of surfactant plugs for single tube experiments and in the $z = 5$ airways of the eight-generation model for each aliquot. For single tube models of $z = 0$–4, we propagated the first aliquot through the airway at $\alpha = 0$ deg, followed by the second aliquot over the pre-existing surfactant film. The volume loss decreased significantly from the first to the second aliquot for $z = 0$–4 ($p < 0.05$). For example, there was a 2.0-fold decrease in the volume loss for the tracheal tube (Fig. 6).

For the multigeneration model, we positioned the airway tree at three different orientations of $\alpha = 0$ deg, 30 deg, and 90 deg, delivered the first aliquot, and then positioned the model at $\alpha = 0$ deg, − 30 deg, and − 90 deg for the second aliquot. Each instilled plug was 140 μL and propagated at Ca = 0.016. Following the first aliquot experiment, we used mild suctioning to remove any surfactant boli in end tubes before administering the second aliquot. The pre-existing surfactant film from the first aliquot made it difficult to form a plug in the tracheal tube with the second aliquot and caused the surfactant solution to spill downstream instead of forming a plug. To mitigate this issue, we placed the plug inside the end of the Tygon tubing that connected to the tracheal tube. The pre-existing surfactant film from the first aliquot also created a glare on the airway walls that limited proper imaging of the second plug. To resolve this issue, we added 2 μL of a red food-coloring dye to the second aliquot before forming the plug inside the Tygon tubing (Movie S5 available in the Supplemental Materials on the ASME Digital Collection). This approach was necessary to quantify the efficiency index using plug volumes.

At $\alpha = 0$ deg, the first aliquot gave $\eta = 42.0\% \pm 0.4$, similar to that from the single dose experiment. We kept the model at this position for the second aliquot to simulate keeping the infant on its back. Our analysis gave a $\eta = 63.7\% \pm 1.7$ for the second aliquot (Movie S4 and S5 available in the Supplemental Materials on the ASME Digital Collection and Fig. 7), i.e., a significant 1.5-fold increase from the first aliquot ($p < 0.05$). Therefore, a pre-existing surfactant film led to a significantly higher volume from a subsequent aliquot to reach lower airways due to a decrease in the deposited volume (Fig. 7). Next, we positioned the airway tree at roll angles of 90 deg and −90 deg for the two-aliquot delivery experiment to mimic rolling the neonate to the left and right sides (Movies S6 and S7 available in the Supplemental Materials). Our analysis showed similar efficiency indices of 61.0% ± 1.6 and 60.9% ± 1.7 for the first and second aliquots, respectively. The higher efficiency from the first aliquot in this orientation than in $\alpha = 0$ deg is because surfactant plugs travel fewer airways (only those in one lung) and lose less mass on airway walls. This is major benefit, but it is important to note that with rotating the airways between the two aliquots, the UR and UL lobes receive ∼100% of the surfactant solution from the two aliquots, whereas the LR and LL lobes receive almost no surfactant (Fig. 7).

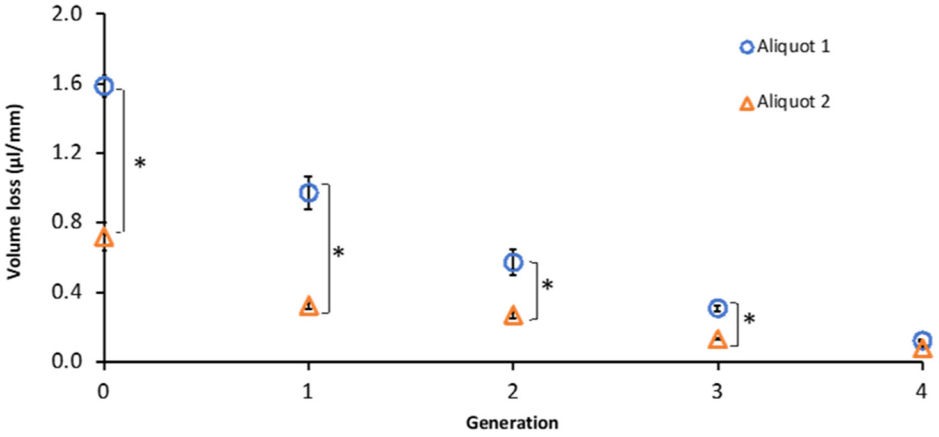

Fig. 6 Volume loss from surfactant plugs in aliquot 2 propagating in single airway tubes representing airway generations $z = 0$, 1, 2, 3, and 4 and traveling over a pre-existing surfactant film deposited from aliquot 1. Each airway tube was 50 mm in length but with a similar diameter to its corresponding airway tube in the multigeneration model. *$p < 0.05$.

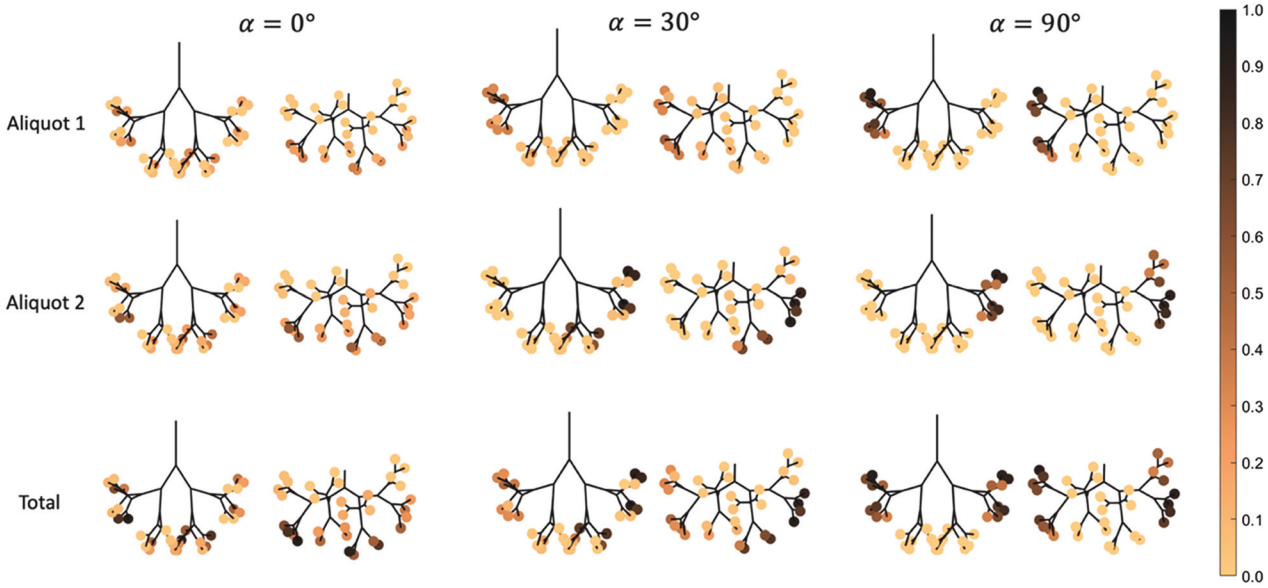

Fig. 7 Heatmaps representing surfactant distribution through the airway tree into the $z = 5$ generation airways in two-aliquot experiments and under different orientations. The $z = 5$ airways are represented as colored spheres and the color bar shows the normalized surfactant solution volume in $z = 5$ airways.

Therefore, although the 90 deg and – 90 deg rotations yield higher efficiency indices, only airways of one lobe in each lung receive surfactant.

Based on the above result that a pre-existing surfactant film significantly increases the delivery efficiency and the importance of delivery of surfactant to the entire lung, we hypothesized that rolling the model at 30 deg and – 30 deg may result in an improved efficiency index while delivering surfactant to all four lobes. The first aliquot at $\alpha = 30$ deg gave $\eta = 41.2\% \pm 1.8$, i.e., similar to that from the $\alpha = 0$ deg experiment. For the second aliquot at $\alpha = -30$ deg, η increased significantly to $61.0\% \pm 4.0$, i.e., 1.5-fold increase than that in the first aliquot. This result was similar to that of the supine position and therefore, this orientation did not provide any further benefit.

Discussion

We presented an experimental study of surfactant transport in a symmetric, eight-generation model of neonates' lung airway tree [1,11,25]. We investigated the distribution of instilled surfactant solution boli in airways and the delivery efficiency to lower airways as a function of orientation of the airway tree. We defined two metrics, distribution index, and efficiency index, to evaluate how orientation of airways in the gravitational field impacts surfactant transport in the lungs. The distribution index helped quantify surfactant delivery to the UR, LR, LL, and UL lobes and within the right and left lungs. The change in distribution index between the four lobes was consistent with previous findings, indicating that the gravitationally favored airways proportionally receive a greater amount of surfactant [15]. For example, changing the roll angle from $\alpha = 0$ deg to $\alpha = 90$ deg to the right increased the distribution index for the UR lobe significantly by 3.25-fold and decreased it for the UL lobe by 16.7-fold.

An important consideration in surfactant replacement therapy (SRT) is to ensure that the instilled surfactant solution reaches lower airways such that surface tension gradients further drain it toward alveoli [22,32]. We studied this question using an efficiency index that quantifies how much of the instilled volume reaches the $z = 5$ airway tubes. While our model contained airways down to $z = 7$, imaging of all airways in generations 6 and 7 in the 3D space within the timeframe of an experiment was not feasible. As such, we quantified surfactant plug sizes in the $z = 5$

airways. The efficiency index of the single aliquot delivery showed the greatest change from $\alpha = 0$ deg to $\alpha = 90$ deg with a 1.4-fold increase. This suggests that positioning an infant completely on their right side increases surfactant volume in the UR lobe and that this orientation may be ideal for SRT. This is consistent with a previous computational study that showed a greater amount of surfactant is delivered to the gravitationally favored lung [15].

A significant finding of our study was that a pre-existing surfactant film in airways significantly improves the efficiency of a subsequent delivery. We demonstrated this using a two-aliquot delivery method. The surfactant plugs from the first aliquot propagated within airways prewetted with a buffer and left behind a surfactant film on airway walls. Propagating the plugs from the second aliquot greatly reduced film deposition in airway tubes [33], transporting surfactant further downstream. As a result, this approach led to a significantly higher delivery efficiency than the single-aliquot approach did. From a practical standpoint, this result suggests dividing the therapeutic dose into two or more aliquots to increase the efficiency of surfactant transport to the respiratory zone of the lung. Because plugs retained a higher volume when flowing through airways containing a surfactant film, the number of airways receiving surfactant also increased.

While a high efficiency index with both aliquots at $\alpha = 90$ deg may suggest that this orientation is optimal for SRT, our results indicate that a supine position provides greater benefits. This is because at $\alpha = 0$ deg, airways from both anterior and posterior of all four lobes received surfactant, whereas at $\alpha = 90$ deg only the anterior and posterior airways of the UR and LR lobes received surfactant. With our model that contains 255 airway tubes, the first and second aliquots, respectively, covered 209 and 229 airways at $\alpha = 0$ deg but only 68 and 67 airways at $\alpha = 90$ deg. In a supine position, the cumulative volume of surfactant solution in the $z = 5$ airways from both aliquots was 131 μL, whereas at $\alpha = 90$ deg, the respective volume was 150 μL. The smaller volume in $z = 5$ airways in the supine position is due to traveling of plugs through more airways and depositing a film on airway walls. Due to covering more airways in the $\alpha = 0$ deg orientation, using a larger instilled volume to enhance surfactant delivery to the respiratory zone is feasible. On the other hand, using larger instilled volumes in the $\alpha = 90$ deg orientation may flood the airways. In practice, keeping preterm infants in a supine position, rather than repositioning them for a subsequent aliquot, simplifies the procedure [34].

From a methodological viewpoint, our study presents a major advance by providing a novel airway model where the size, bifurcations, and 3D rotations of airways in the gravitational field closely mimic those of native lung airways. Although the Young modulus of the material is larger than that of conducting zone airways ($E \sim 10$ MPa) [35,36], these airways in infants or adults are significantly less compliant than those in the respiratory zone due to the surrounding cartilage from fetal development [1,37]. We ensured this through image analysis of airways of excised rat lungs under SRT that did not show a detectable change during ventilation [38]. Thus, the stiffness difference between airways of our model and native airways is unlikely to impact surfactant deposition or distribution in conducting airways. A complexity of native airways that our model excludes is the presence of an epithelium lining covered with a thin aqueous film [2]. To address this, we prewetted the interior of the airways by running a plug of a buffer solution through the model to leave a thin film behind. We found that presence of epithelium under the aqueous film does not alter film deposition from propagating surfactant plugs (data not shown). However, the aqueous layer significantly changed the deposited mass compared to dry walls used in previous studies.

Our engineered 3D airway model is a new tool to study fluid flow in airways but still requires several improvements to more closely mimic human lungs and clinical SRT. Our future quantitative studies of surfactant transport in the engineered airway tree model will consider several major parameters including asymmetry of left and right lungs and their bifurcating airways, a five lobe lung design that is physiologically more relevant to human lungs, and cyclic ventilation effects on propagation of surfactant plugs and film deposition onto airway walls. In addition, our current model did not incorporate the compliance of pulmonary acini and its potential effects on surfactant transport in airways. We envision designing and implementing compliant enclosures in the terminal airways to investigate to what extent the resulting pressure difference across propagating plugs in conjunction with cyclic airflow affect processes such as splitting of plugs at bifurcations, film deposition on airway walls, formation of secondary plugs, and ultimately distribution of instilled surfactant. Finally, a better imaging system will enable more detailed imaging of surfactant transport in the 3D space in airways. Overall, this basic research study provides the framework to develop more complex models that facilitate translational studies.

Conclusion

We developed a 3D physical model of the conducting zone of the tracheobronchial tree of preterm infants to quantitatively study surfactant transport into the lungs during NSRT. Our study showed that gravitational orientation of the lungs during a single aliquot delivery significantly impacts the distribution of surfactant to airways of different lobes. Gravitationally favored airways proportionally received more surfactant. Additionally, we found that when two aliquots are instilled, the efficiency of surfactant delivery increases significantly because a pre-existing surfactant film from the first aliquot reduces film deposition from the second aliquot and enables transport of the surfactant solution further down the airway tree. Our findings suggest that a supine position may be ideal to ensure delivery of surfactant to anterior and posterior airways of all four lobes with a high efficiency while avoiding complexities and potential risks of rotating the neonate between different aliquots during NSRT. Our approach to design and fabricate 3D biomimetic lung airway tree models will enable future studies of transport of different therapeutics in the forms of boli or aerosols.

Funding Data

- National Science Foundation (Grant Nos. 1904204 and 1904210; Funder ID: 10.13039/100000001).

Conflict of Interest

There are no conflicts of interest.

References

[1] Weibel, E. R., and Gomez, D. M., 1962, "Architecture of the Human Lung: Use of Quantitative Methods Establishes Fundamental Relations Between Size and Number of Lung Structures," Science, **137**(3530), pp. 577–585.

[2] West, J. B., and Luks, A., 2016, West's Respiratory Physiology: The Essentials, Wolters Kluwer, Philadelphia, PA, p. 238.

[3] Andreeva, A. V., Kutuzov, M. A., and Voyno-Yasenetskaya, T. A., 2007, "Regulation of Surfactant Secretion in Alveolar Type II Cells," Am. J. Physiol.-Lung Cell. Mol. Physiol., **293**(2), pp. L259–L271.

[4] Banaschewski, B. J. H., Veldhuizen, E. J. A., Keating, E., Haagsman, H. P., Zuo, Y. Y., Yamashita, C. M., and Veldhuizen, R. A. W., 2015, "Antimicrobial and Biophysical Properties of Surfactant Supplemented With an Antimicrobial Peptide for Treatment of Bacterial Pneumonia," Antimicrob. Agents Chemother., **59**(6), pp. 3075–3083.

[5] Tavana, H., Huh, D., Grotberg, J. B., and Takayama, S., 2009, "Microfluidics, Lung Surfactant, and Respiratory Disorders," Lab. Med., **40**(4), pp. 203–209.

[6] Veldhuizen, E. J. A., and Haagsman, H. P., 2000, "Role of Pulmonary Surfactant Components in Surface Film Formation and Dynamics," Biochim. Biophys. Acta, **1467**(2), pp. 255–270.

[7] Colin, A. A., McEvoy, C., and Castile, R. G., 2010, "Respiratory Morbidity and Lung Function in Preterm Infants of 32 to 36 Weeks' Gestational Age," Pediatrics, **126**(1), pp. 115–128.

[8] Hamvas, A., 1997, "Surfactant Protein B Deficiency: Insights Into Inherited Disorders of Lung Cell Metabolism," Curr. Probl. Pediatr., **27**(9), pp. 325–345.

[9] Polin, R. A., Carlo, W. A., Papile, L.-A., Polin, R. A., Carlo, W., Tan, R., Kumar, P., Benitz, W., Eichenwald, E., Cummings, J., and Baley, J., Committee on Fetus and Newborn, 2014, "Surfactant Replacement Therapy for Preterm and Term Neonates With Respiratory Distress," Pediatrics, **133**(1), pp. 156–163.

[10] Stevens, T. P., and Sinkin, R. A., 2007, "Surfactant Replacement Therapy," Chest, **131**(5), pp. 1577–1582.
[11] Copploe, A., Vatani, M., Amini, R., Choi, J.-W., and Tavana, H., 2018, "Engineered Airway Models to Study Liquid Plug Splitting at Bifurcations: Effects of Orientation and Airway Size," ASME J. Biomech. Eng., **140**(9), p. 091012.
[12] Espinosa, F. F., and Kamm, R. D., 1999, "Bolus Dispersal Through the Lungs in Surfactant Replacement Therapy," J. Appl. Physiol., **86**(1), pp. 391–410.
[13] Corbet, A., Bucciarelli, R., Goldman, S., Mammel, M., Wold, D., and Long, W., 1991, "Decreased Mortality Rate Among Small Premature Infants Treated at Birth With a Single Dose of Synthetic Surfactant: A Multicenter Controlled Trial," J. Pediatr., **118**(2), pp. 277–284.
[14] Wood, A. J. J., and Jobe, A. H., 1993, "Pulmonary Surfactant Therapy," N. Engl. J. Med., **328**(12), pp. 861–868.
[15] Filoche, M., Tai, C.-F., and Grotberg, J. B., 2015, "Three-Dimensional Model of Surfactant Replacement Therapy," Proc. Natl. Acad. Sci., **112**(30), pp. 9287–9292.
[16] Davis, D. J., and Barrington, K. J., Canadian Paediatric Society, and Fetus and Newborn Committee, 2005, "Paediatrics Child Health. Recommendations for Neonatal Surfactant Therapy," Can. Paediatr. Soc., **10**(2), pp. 346–361.
[17] Robertson, B., and Halliday, H. L., 1998, "Principles of Surfactant Replacement," Biochim. Biophys. Acta BBA Mol. Basis Dis., **1408**(2–3), pp. 346–361.
[18] Zola, E. M., Gunkel, J. H., Chan, R. K., Lim, M. O., Knox, I., Feldman, B. H., Denson, S. E., Stonestreet, B. S., Mitchell, B. R., Wyza, M. M., Bennett, K. J., and Gold, A. J., 1993, "Comparison of Three Dosing Procedures for Administration of Bovine Surfactant to Neonates With Respiratory Distress Syndrome," J. Pediatr., **122**(3), pp. 453–459.
[19] Rojas-Reyes, M. X., Morley, C. J., and Soll, R., 2012, "Prophylactic Versus Selective Use of Surfactant in Preventing Morbidity and Mortality in Preterm Infants," Cochrane Database Syst. Rev., (3), Article No. CD000510.
[20] Hentschel, R., Bohlin, K., van Kaam, A., Fuchs, H., and Danhaive, O., 2020, "Surfactant Replacement Therapy: From Biological Basis to Current Clinical Practice," Pediatr. Res., **88**(2), pp. 176–183.
[21] Fujioka, H., Takayama, S., and Grotberg, J. B., 2008, "Unsteady Propagation of a Liquid Plug in a Liquid-Lined Straight Tube," Phys. Fluids, **20**(6), p. 062104.
[22] Tavana, H., Kuo, C.-H., Lee, Q. Y., Mosadegh, B., Huh, D., Christensen, P. J., Grotberg, J. B., and Takayama, S., 2010, "Dynamics of Liquid Plugs of Buffer and Surfactant Solutions in a Micro-Engineered Pulmonary Airway Model," Langmuir, **26**(5), pp. 3744–3752.
[23] Zheng, Y., Anderson, J. C., Suresh, V., and Grotberg, J. B., 2005, "Effect of Gravity on Liquid Plug Transport Through an Airway Bifurcation Model," ASME J. Biomech. Eng., **127**(5), pp. 798–806.
[24] Zheng, Y., Fujioka, H., Grotberg, J. C., and Grotberg, J. B., 2006, "Effects of Inertia and Gravity on Liquid Plug Splitting at a Bifurcation," ASME J. Biomech. Eng., **128**(5), pp. 707–716.
[25] Copploe, A., Vatani, M., Choi, J.-W., and Tavana, H., 2019, "A Three-Dimensional Model of Human Lung Airway Tree to Study Therapeutics Delivery in the Lungs," Ann. Biomed. Eng., **47**(6), pp. 1435–1445.
[26] Emadeldin, B., and Abukonna, A., 2016, "Estimation of Radiation Dose in the Neonatal Intensive Care Unit (NICU)," J. Med. Phys. Appl. Sci., **1**(2), pp. 1–3.
[27] Kitaoka, H., Takaki, R., and Suki, B., 1999, "A Three-Dimensional Model of the Human Airway Tree," J. Appl. Physiol., **87**(6), pp. 2207–2217.
[28] Bretherton, F. P., 1961, "The Motion of Long Bubbles in Tubes," J. Fluid Mech., **10**(02), p. 166.
[29] Aussillous, P., and Quéré, D., 2000, "Quick Deposition of a Fluid on the Wall of a Tube," Phys. Fluids, **12**(10), p. 2367.
[30] Nouraeyan, N., Lambrinakos-Raymond, A., Rrt, M. L., and Frcpc, G. S., 2014, "Surfactant Administration in Neonates: A Review of Delivery Methods," Can. J. Respir. Ther., **50**(3), pp. 91–95.
[31] Speer, C. P., Gefeller, O., Groneck, P., Laufkotter, E., Roll, C., Hanssler, L., Harms, K., Herting, E., Boenisch, H., and Windeler, J., 1995, "Randomised Clinical Trial of Two Treatment Regimens of Natural Surfactant Preparations in Neonatal Respiratory Distress Syndrome," Arch. Dis. Child. Fetal Neonatal Ed., **72**(1), pp. F8–13.
[32] Grotberg, J. B., 2001, "Respiratory Fluid Mechanics and Transport Processes," Annu. Rev. Biomed. Eng., **3**(1), pp. 421–457.
[33] Halpern, D., Jensen, O. E., and Grotberg, J. B., 1998, "A Theoretical Study of Surfactant and Liquid Delivery Into the Lung," J. Appl. Physiol., **85**(1), pp. 333–352.
[34] Kendig, J. W., Ryan, R. M., Sinkin, R. A., Maniscalco, W. M., Notter, R. H., Guillet, R., Cox, C., Dweck, H. S., Horgan, M. J., Reubens, L. J., Risemberg, H., and Phelps, D. L., 1998, "Comparison of Two Strategies for Surfactant Prophylaxis in Very Premature Infants: A Multicenter Randomized Trial," Pediatrics, **101**(6), pp. 1006–1012.
[35] Lambert, R. K., Baile, E. M., Moreno, R., Bert, J., and Pare, P. D., 1991, "A Method for Estimating the Young's Modulus of Complete Tracheal Cartilage Rings," J. Appl. Physiol., **70**(3), pp. 1152–1159.
[36] Trabelsi, O., del Palomar, A. P., López-villalobos, J. L., Ginel, A., and Doblaré, M., 2010, "Experimental Characterization and Constitutive Modeling of the Mechanical Behavior of the Human Trachea," Med. Eng. Phys., **32**(1), pp. 76–82.
[37] Szpinda, M., Daroszewski, M., Woźniak, A., Szpinda, A., and Mila-Kierzenkowska, C., 2012, "Tracheal Dimensions in Human Fetuses: An Anatomical, Digital and Statistical Study," Surg. Radiol. Anat., **34**(4), pp. 317–323.
[38] Cassidy, K. J., Bull, J. L., Glucksberg, M. R., Dawson, C. A., Haworth, S. T., Hirschl, R., Gavriely, N., and Grotberg, J. B., 2001, "A Rat Lung Model of Instilled Liquid Transport in the Pulmonary Airways," J. Appl. Physiol., **90**(5), pp. 1955–1967.